# Faulting structure above the Main Himalayan Thrust as shown by relocated aftershocks of the 2015 $M_W 7.8$ Gorkha, Nepal earthquake

Ling Bai[1], Hongbing Liu[1], Jeroen Ritsema[2], James Mori[3], Tianzhong Zhang[4], Yuzo Ishikawa[5], and Guohui Li[1]



Three key points:

(1) We relocate the 2015 Gorkha earthquakes using teleseismic and regional waveforms.

(2) The mainshock is located on the horizontal Main Himalaya Thrust (MHT) at a depth of 18.5 km.

(3) Aftershocks show faulting structure in the hanging wall above the MHT.

[1]Key Laboratory of Continental Collision and Plateau Uplift, Institute of Tibetan Plateau Research, Chinese Academy of Sciences, Beijing, China.
(bailing@itpcas.ac.cn)

[2]Department of Earth and Environmental Sciences, University of Michigan, Ann Arbor, Michigan, USA.

[3]Disaster Prevention Research Institute, Kyoto University, Uji, Kyoto, Japan.

[4]Institute of Geophysics, China Earthquake Administration, Beijing, China.

[5]National Institute of Advanced Industrial Science and technology, Tsukuba, Japan.

The 25 April 2015, $M_W$ 7.8 Gorkha, Nepal earthquake ruptured a shallow section of the Indian-Eurasian plate boundary by reverse faulting with NNE-SSW compression, consistent with the direction of current Indian-Eurasian continental collision. The Ghorka mainshock and aftershocks were recorded by permanent global and regional arrays and by a temporary local broadband array near the China-Nepal border deployed prior to the Ghorka mainshock. We relocate 272 earthquakes with $M_W > 3.5$ by applying a multi-scale double-difference earthquake relocation technique to arrival times of direct and depth phases recorded globally and locally. We determined a well-constrained depth of 18.5 km for the mainshock hypocenter which places it on the Main Himalayan Thrust (MHT). Many of the aftershocks at shallower depths illuminate faulting structure in the hanging wall with dip angles that are steeper than the MHT. This system of thrust faults of the Lesser Himalaya may accommodate most of the elastic strain of the Himalayan orogeny.

## 1. Introduction

The collision between the Indian and Eurasian continental plates formed the Himalaya mountain range, the highest orogenic belt on Earth with widespread continental seismicity. The region is classically divided into four tectonic units from south to north: sub-Himalaya, Lesser Himalaya, Higher Himalaya and Tethyan Himalaya [**?**] (Figure 1). The Main Frontal Thrust (MFT), Main Boundary Thrust (MBT), Main Central Thrust (MCT), and South Tibet Detachment (STD) separate the four tectonic units. They converge at the Main Himalaya Thrust (MHT), the detachment along which the Indian plate subducts beneath the Himalayan mountains [**???**].

The potential for devastating earthquakes in the Himalaya has long been recognized. Historical documents since the $10^{th}$ century show evidence for great Himalayan earthquakes with a recurrence interval of about 800 years [**??**]. Nearly 500 earthquakes of $M_W \geq 4.5$ have occurred along the Himalayas orogen since 1964. The Gorkha, Nepal earthquake has heightened concern for large earthquakes along the Himalayan front [**??**]. This is the first well-recorded earthquake and aftershock sequence on the shallowest portion of the MHT. The seismic data will provide new constraints on the fault zone structure of the Indian-Eurasian plate boundary at shallow depth and insight into seismic hazard in the region.

In this study, we relocate aftershock hypocenters to infer the structure of the Gorkha earthquake fault zone. Our data come from the Global Seismic Network, the China National Seismic Network, and a temporary array of 15 broadband seismic stations that we deployed at the China-Nepal border in December 2014. The combination of teleseimic

(30–90°) P waveforms and regional Pg, Sg, Pn and Sn signals is optimal for precise hypocenter determinations.

## 2. The Main Himalayan Thrust

The MHT is defined as the detachment that separates the underthrusting Indian plate from the overriding Himalaya orogeny. The concept of the MHT was proposed by **?** based on the locations and fault plane solutions of moderate earthquakes at 10–20 km depths. A similar concept of Main Detachment Fault was put forward by **?** from a tectonic reconstruction of eastern Nepal. The MHT was imaged at a depth of 30–40 km by **?** with a deep seismic reflection profile in southeastern Tibet. In the past decade, broadband seismic arrays have been deployed to constrain the structure of the MHT in the central [**???**], eastern [**??**] and western [**??**] Himalaya, respectively.

Subduction of the Indian continental lithosphere beneath the Himalaya has been shallow and nearly horizontal since initiation of the Indo-Asian collision. The dip angle increases with depth from the MCT to the Indus-Tsangpo suture (ITS). The deeper sections of the MHT are constrained best [e.g., **?**]. However, the shallow structure of the MHT remains uncertain because the interpretation of shallow seismic wave refraction is difficult [**??**].

## 3. Waveform modeling and Multi-DD relocations

We relocated a total of 272 earthquakes, including the Gorkha mainshock, 233 aftershocks within one month and 38 earthquakes that occurred before the Gorkha earthquake since 1980 (Figure 1, and Table S2). Our estimates are based on five data sets: (1) bulletins from the National Earthquake Information Center (NEIC) of the U.S. Geological Survey (USGS) for 234 earthquakes of $M_W > 3.5$ that occurred within one month after

the mainshock, (2) bulletins from the National Seismic Network of Nepal and the International Seismological Centre (ISC) for 38 earthquakes of $M_W > 3.5$ that occurred in the source region during three decades prior to the Ghorka earthquake, (3) seismic and waveform data from the China Earthquake Data Center (CEDC) and the China National Seismic Network (CNSN), (4) teleseismic P waveforms from the Global Seismic Network, and (5) waveform data from a temporary array of 15 broadband seismic stations along the China-Nepal border, deployed by the Institute of Tibetan Plateau Research, Chinese Academy of Sciences prior to the Gorkha earthquake. Our local temporary array recorded many of the aftershocks at epicentral distances less than 100 km (Figure 2 (a)), including the $M_W > 7.3$ Kodari earthquake [**?**]. Permanent seismic stations in the Tibetan region at epicentral distances of 2–7° recorded clear Pn and Sn head waves and Pg and Sg waves (Figure 2 (b)). At teleseismic distances, surface reflections pP and sP phases for moderate earthquakes (Figure 3) provide constraints on focal depths.

Our analysis comprises three steps. First we determine hypocenters for the Gorkha earthquake and its 233 aftershocks based on the HYPOSAT methodology [**?**]. Absolute traveltimes and traveltime differences at common stations are modeled using a layered velocity structure in the source region, representing the Himalayan orogenic prism, the Indian upper and lower crust, and the Indian mantle, respectively [**???**] (Table S1). We constrain the absolute focal depths of moderate aftershocks ($M_W$ 5.5 to $M_W$ 6.3, Table S2) by modeling the teleseismic waveforms of the direct P and the surface reflections pP and sP (Figure 3) following **?**. Using the depths determined by HYPOSAT and by waveform modeling, we calculate hypocenters of all earthquakes using a multi-scale

double-difference earthquake relocation method (Multi-DD) [**?**], which is modified from the hypoDD programs [**?**] to include phases recorded by regional and teleseismic networks. Since differential traveltimes do not depend strongly on the assumed velocity models along the whole raypath [**??**], the joint analysis of local, regional and teleseismic data and the precise measurements of differential phase arrival times via waveform cross correction for the China-Nepal array ((Figure S1)) improve the relative focal depth determinations considerably. The focal depths for earthquakes determined by waveform modeling are held fixed during the Multi-DD processing to constrain the absolute focal depths of all earthquakes. We calculate differential traveltimes between each event and up to eight of its nearest neighbors. Each event pair has 8–32 commonly observed phases within a 15 km distance between the two events. The data include 9,690 Pg and Sg, 5,288 Pn and Sn, 174 pP and sP, and 17,664 teleseismic P and S arrival times.

## 4. Results

We estimated the uncertainty of the relocations by a bootstrap analysis [**?**] using 100 sampling iterations (Figure S2). This analysis indicates that epicenters are estimated with an accuracy of ±3.5 km, which is two times smaller than the average uncertainty of ±7.0 km reported in the NEIC catalog. The uncertainty in the focal depth estimate is ±2.0 km, in agreement with the estimates of focal depth uncertainty based on waveform fits (Figure 3). The differential time residuals are reduced substantially from ±5 s before to ±1.5 s after relocations (Figure S3). The weighted L1 and L2 norm residuals decreased from 1.10 s and 1.58 s to 0.46 s and 0.60 s after relocations, respectively, demonstrating that the earthquakes are better relocated.

On average, the epicenters have been relocated by 6.2 km. The average focal depth after relocation is 14.7 km below the surface, deeper than the default value of 10 km in the NEIC catalog for most of the aftershocks. Almost all aftershocks occurred to the southeast of the mainshock. Few aftershocks occurred northeast of Kathmandu, where coseismic slip is large [?????]. The $M_W$ 7.3 Kodari earthquake occurred on the eastern edge of the aftershock zone. We estimate the focal depth of the mainshock to be 18.5±2 km (Figure 3), consistent with the depth of the MHT [?] and the locking line at the source region [??]. The focal depths of the $M_W$ 7.3 and $M_W$ 6.7 aftershocks (events 150 and 86 in Table S2) are 21 km, slightly deeper than the depth of MHT near a patch of large slip below the plate surface [?].

Figure 4 shows relocated hypocenters of the mainshock and major aftershocks along a N20°E cross-section perpendicular to the strike of the Ghorka mainshock fault plane. Most aftershocks are shallower than the mainshock and located in the hanging wall. They line up as clear north-dipping structures with dip angles of about 25°, which is 15° steeper than the dip of the MHT [?] and the shallow nodal plane of the mainshock [?]. The steeper dips are in good agreement with the focal mechanisms solutions of aftershocks 12, 76, 98, 156, and 222 (Table S2) reported in the global Centroid Moment Tensor (gCMT) catalog.

## 5. Discussion and conclusions

The 2015 Ghorka earthquake sequence on a shallow section of the MHT has been recorded extremely well by local, regional, and global seismic arrays. From precise relocations, we infer that the Gorkha aftershocks (Figure 1) are distributed above the anticlinorium system of the MCT. The southern edge of the aftershock zone is very close

to the MBT [?], which is the thrust placing the lesser Himalaya over Tertiary sedimentary strata. ? suggested that earthquakes along Himalaya orogeny are mostly parallel to the MBT. These observations indicate that the MBT may be important in controlling earthquake occurrence along the frontal edge of the Himalaya.

While the mainshock ruptured a section of the MHT, most of the aftershocks with $M_W$ 3.5 or larger have shallower focal depths and the northward dipping nodal planes of the largest aftershocks have larger dip angles. We infer therefore that the aftershocks are mainly distributed on steeper dipping structures within the hanging wall of the Lesser Himalaya (Figure 4).

Northward motion on the Indian plate was associated with development of a thrust system that consists of both the near horizontal MHT and more steeply dipping faults above. ? and ? suggested such Lesser Himalayan duplex system to exist in the western Himalaya and to cause folding of the MCT and STD at deeper depth. The Ghorka aftershock locations indicates that this thrust system is also present in central Nepal.

Active faults exist throughout the Kathmandu basin [?]. However, strike-slip earthquakes on these near-vertical faults have not been recorded in the past fifty years [?]. Great earthquakes in the past 200 years include the August 26, 1833 $M_W$ 8.0 event [?], and the January 15, 1934 $M_W$ 8.0 Bihar-Nepal event [?] (Figure 1), which have been attributed to slip on the MHT. Many of the historical large earthquakes along the Himalaya orogeny were located beneath the Lesser Himalaya [?]. We infer that the Lesser Himalaya thrust system is the most seismically active region along the Himalaya convergence and accommodates most of the elastic strain accumulation of the region.

**Acknowledgments.** This research is funded by the grants of National Nature Science Foundation of China (41274086, 41490615) and the Chinese Academy of Sciences (CAS: L. Bai) to LB, the grant of National Nature Science Foundation of China (41174069) to HL, and the grant of National Science Foundation of U.S. (EAR-1416695) to JR. We used Earthquake catalogs from the reviewed ISC bulletin, CEDC, and NEIC, and waveform data from the Data Management Center of IRIS and CNSN at Institute of Geophysics, China Earthquake Administration (SEISDMC, doi: 10.7914/SN/CB, [**?**]), respectively. We are grateful to the China-Nepal array team for conducting the field work.

**Figure 1.** The study region showing the relocations of the $M_W$7.8 Gorkha, $M_W$7.3 Kodari earthquakes (yellow starts), aftershocks (red circles) and earthquakes that occurred before the Gorkha earthquake since 1980 (blue circles) superposed on a slip model [**?**]. Historic seismicity of $M_W > 7.0$ since 1000 is shown with large black circles. Blue triangles show the 15 stations of the China-Nepal seismograph array deployed before the Gorkha earthquake. Green triangles show the short period seismic stations of the National Seismic Network of Nepal. Station EVN and ZBA belong to the IO and CEDC networks, respectively. The black square shows the location of Nepal's capital city, Kathmandu. The double lines indicate the location and the direction N20°E of the cross section shown in Figure 4. The inset at the lower left corner shows seismic stations from the China National Seismic Network (green triangles) and the Global Seismic Network (black triangles) used in this study.

**Figure 2.** Record section of vertical-component seismograms for event 222 (Table S2) recorded by the (a) China-Nepal array and (b) China National Seismic Network. Dotted red lines are observed arrival times of each phase.

**Figure 3.** Comparison of the recorded (thick lines) and computed P waveform for event 98 (Table S2) at stations (a) TIXI, (b) JSD, and (c) KIV. Waveforms are bandpass filtered from 0.01 to 1 HZ. The preferred focal depth for this event is 15.5 km below the surface (thin lines) or 14.2 km beneath sea level. Waveform misfit for H = 10 km (0.73) and H = 20 km (0.96) are much higher because pP and sP phases in the data and the computed seismograms are misaligned. (d) Focal mechanism of the earthquake. Locations of the 3 stations shown in (a)-(c) are shown by open circles.

**Figure 4.** Cross section along the double lines in Figure 1 showing relocated earthquakes occurred either before the $M_W$ 7.3 event or after the $M_W$ 7.3 even with magnitudes greater than 5. Yellow and blue earthquake focal mechanisms show events with dip angles of about 10° and 25°, respectively (http://www.globalcmt.org/). Numbers are the earthquake ID (Table S2 in the supplementary material). The dotted black lines indicate the steeply dipping faults where aftershocks occurred within the Lesser Himalayan thrust system.

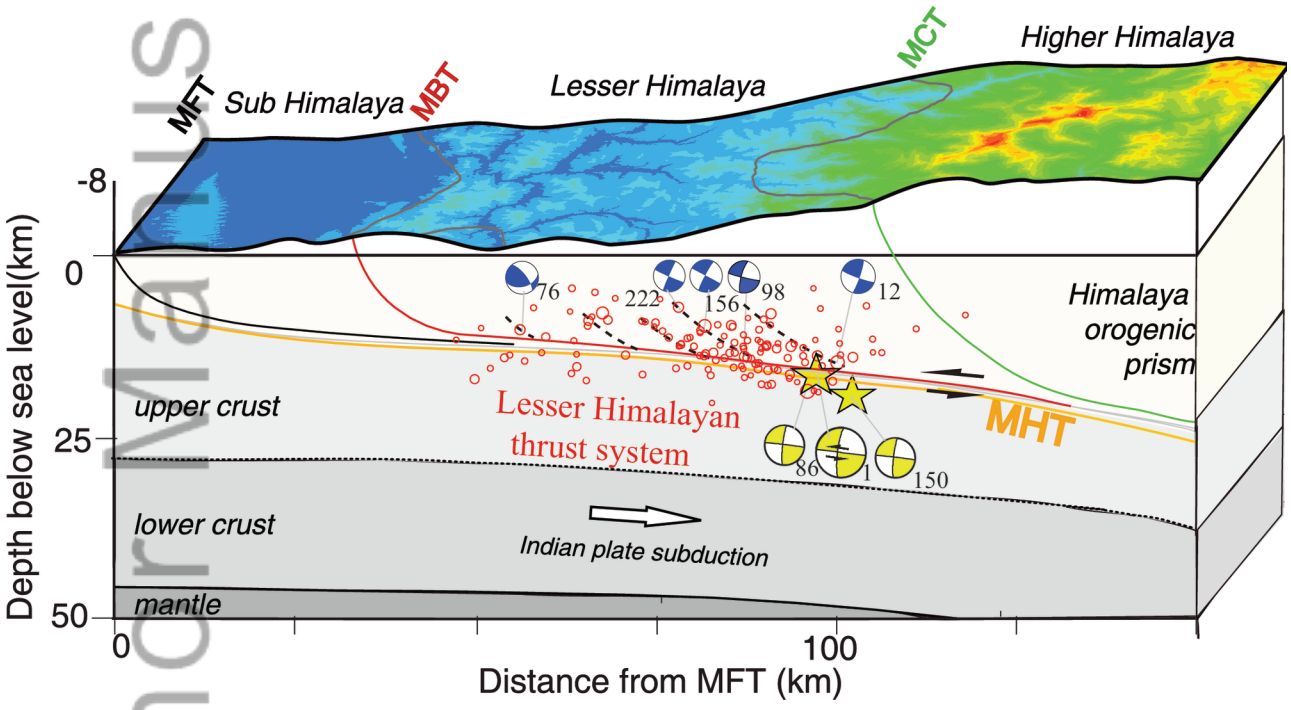


2015gl066473-f00-z-

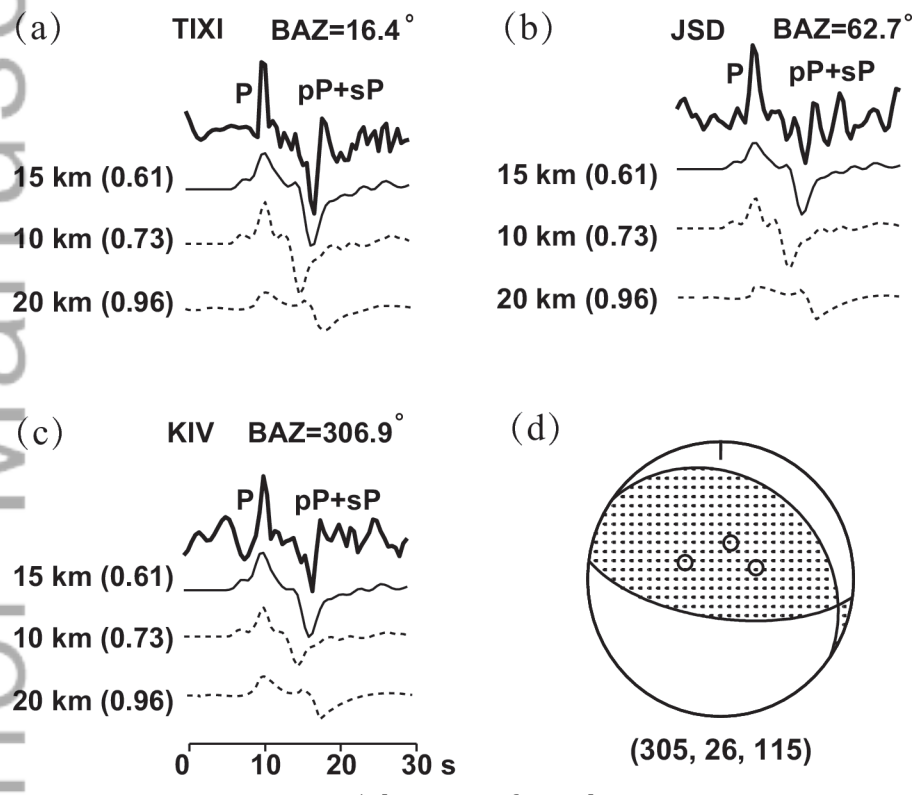


2015gl066473-f01-z-bw

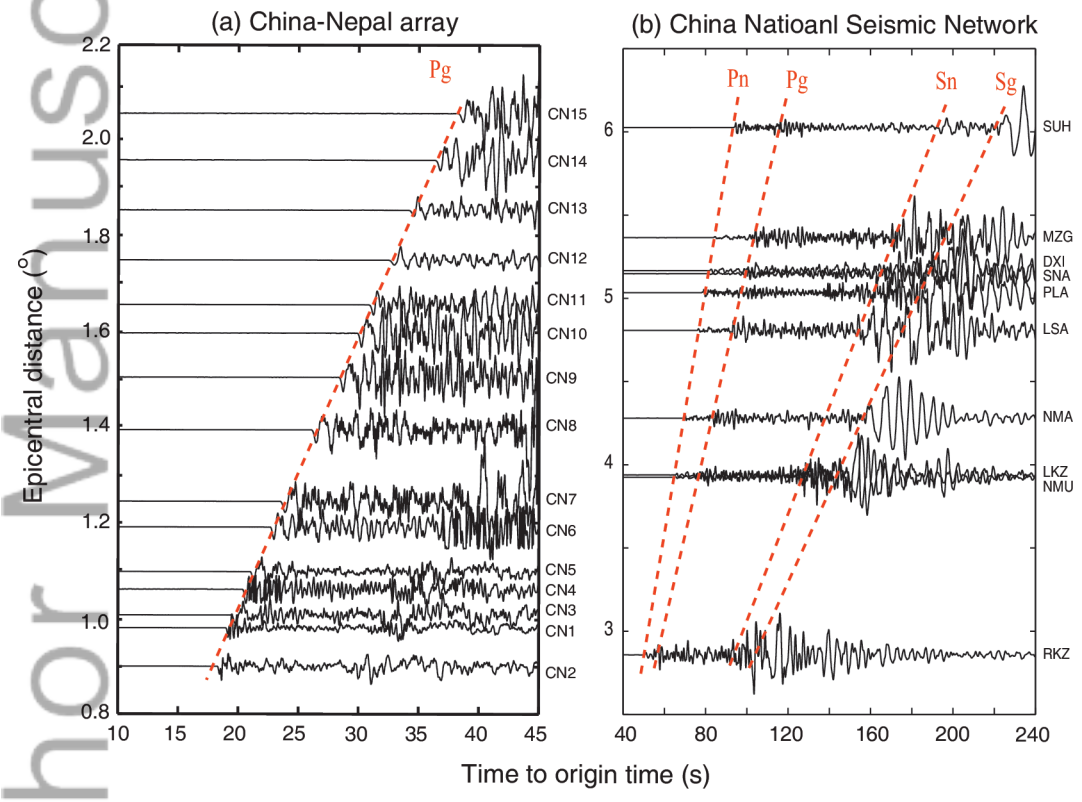


2015gl066473-f02-z-

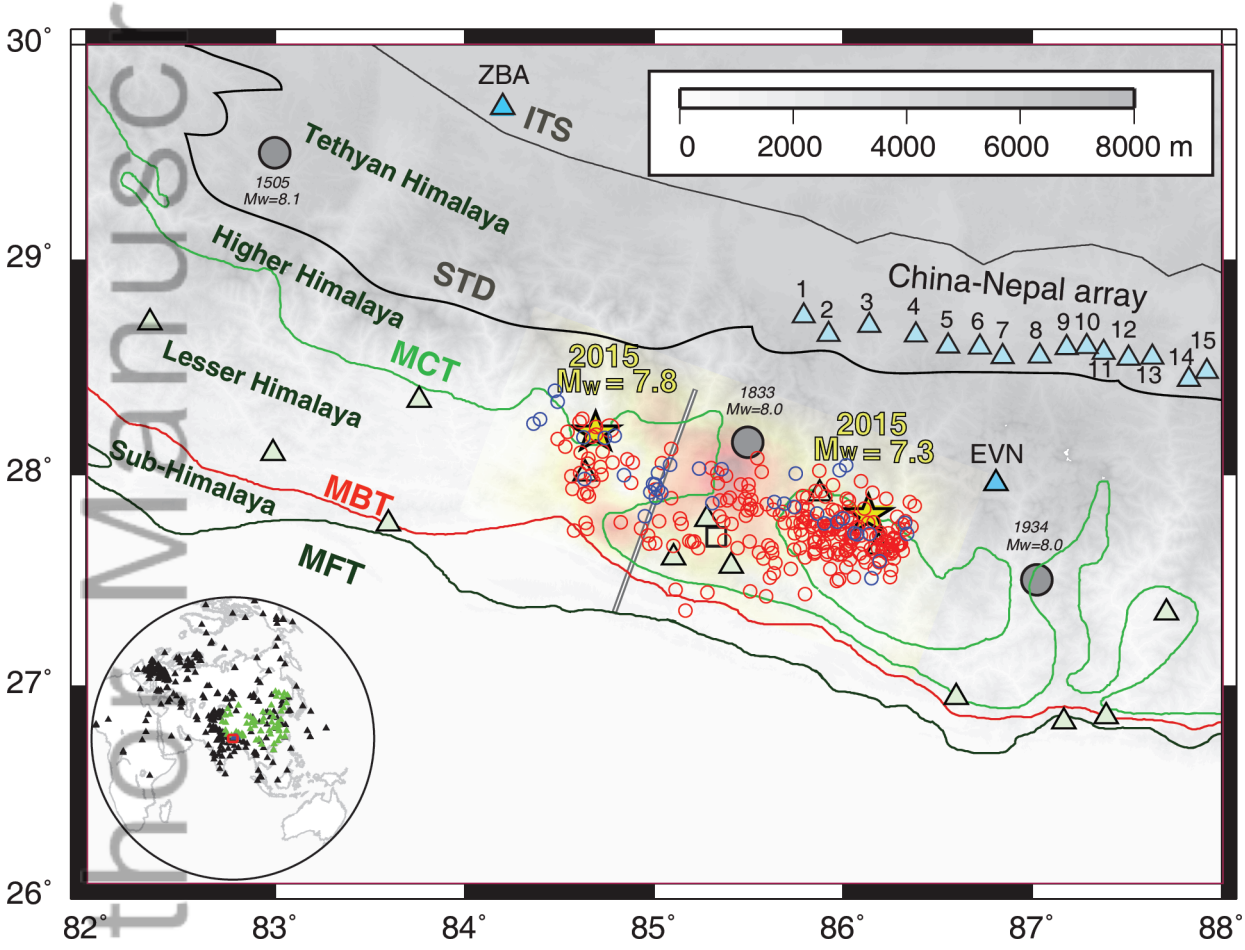


2015gl066473-f03-z-